Optical Design Alternatives: A Survey Study

Ayman Abdel Khader Ismail, A.Prof. Imane Aly Saroit Ismail and Prof. S.H.Ahmed

Information Technology Department, Faculty of Computers & Information, Cairo University

Abstract:

Computers have enhanced human life to a great extent. Our daily lives demand solutions to increasingly sophisticated and complex problems, which requires more speed and better performance of computers. Although the development of the Very Large Scale Integration (VLSI) technology with smaller device dimensions and greater complexity and speed but it does not permits the demand of faster and enhanced computers. Because of the advantages of optical transmission over electronic ones most of researches focused on optical circuit design. In the recent few years, many studies were published in this field. In this paper we will review different methods of optical digital design.

1. Introduction

Computers have enhanced human life to a great extent. The speed of conventional computers is achieved by miniaturizing electronic components to a very small micron-size scale so that those electrons need to travel only very short distances within a very short time. The goal of improving computer speed has resulted in the development of the Very Large Scale Integration (VLSI) technology with smaller device dimensions and greater complexity. Last year, the smallest dimensions of VLSI reached 0.08 mm by researchers at Lucent Technology. Whereas VLSI technology has revolutionized the electronics industry and established the 20th century as the computer age, increasing usage of the Internet demands better accommodation of a 10 to 15 percent per month growth rate. Additionally, our daily lives demand solutions to increasingly sophisticated and complex problems, which requires more speed and better performance of computers. For these reasons, it is unfortunate that VLSI technology is approaching its fundamental limits in the sub-micron miniaturization process [1].

It is now possible to fit up to 300 million transistors on a single silicon chip. It is also estimated that the number of transistor switches that can be put onto a chip doubles every 18 months. Further miniaturization of lithography introduces several problems such as dielectric breakdown, hot carriers, and short channel effects. All of these factors combine to seriously degrade device reliability. Even if developing technology succeeded in temporarily overcoming these physical problems, we will continue to face them as long as increasing demands for higher integration continues. Therefore, a dramatic solution to the problem is needed, and unless we gear our thoughts toward a totally different pathway, we will not be able to further improve our computer performance for the future [1].

Optical interconnections and optical integrated circuits will provide a way out of these limitations to computational speed and complexity inherent in conventional electronics. Optical computers will use photons traveling on optical fibers or thin films instead of electrons to perform the appropriate functions. In the optical computer of the future, electronic circuits and wires will be replaced by a few optical fibers and films, making the systems more efficient with no interference, more cost effective, lighter and more compact [1].

Optical components would not need to have insulators as those needed between electronic components because they don't experience cross talk. Indeed, multiple frequencies (or different colors) of light can travel through optical components without interfering with each others, allowing photonic devices to process multiple streams of data simultaneously. Optical interconnections and optical integrated circuits have several advantageous over their electronic counterparts. They are immune to electromagnetic interference, and free from electrical short circuits. They have low-loss transmission and provide large bandwidth; i.e. multiplexing capability, capable of communicating several channels in parallel without interference. They are capable of propagating signals within the same or adjacent fibers with essentially no interference or cross-talk. They are compact, lightweight, and inexpensive to manufacture, and more facile with stored information than magnetic materials [2].

We are in an era of daily explosions in the development of optics and optical components for computing and other applications. The business of photonics is booming in industry and universities worldwide. It is estimated that photonic device sales worldwide will range between $12 billion and $100 billion. In 1999 due to an ever-increasing demand for data traffic according to KMI corp., data traffic is growing worldwide at a rate of 100% per year, while, the Phillips Group in London estimates that the U.S. data traffic will increase by 300% annually. KMI corp. also estimates that sales of dense-wavelength division multiplexing equipment will increase by more than quadruple its growth in the next five years, i.e. from $2.2 billion worldwide in 1998 to $9.4 billion 2004. In fact, Future Communication Inc., London, announced this year to upgrade their communication system accordingly. The company's goal is to use wavelength division multiplexing at 10 Gb/s/channel to transmit at a total rate of more than 1000 Tb/s [1,2].

Most of the components that are currently in use with very much in demand are electro-optical (EO). Such hybrid components are limited by the speed of their electronic parts. All-optical components will have the advantage of speed over EO components. Unfortunately, there is an absence of known efficient nonlinear optical materials that can respond at low power levels. Most all-optical components require a high level of laser power to function as required. A group of researchers from the University of Southern California, jointly with a team from the University of Los Anglos, have developed an organic polymer with a switching frequency of 60 GHz.

This is three times faster than the current industry standard, lithium niobate crystal-based devices. The California team has been working to incorporate their material into a working prototype. Development of such a device could revolutionize the information superhighway and speed data processing for optical computing [1,2].

Another group at Brown University and the IBM Almaden Research Center (San Jose, CA) has used ultra fast laser pulses to build ultra fast data storage devices. This group was able to achieve ultra fast switching down to 100ps. Their results are almost ten times faster than currently available speed limits. Optoelectronic technologies for optical computers and communication hold promise for transmitting data as short as the space between computer chips or as long as the orbital distance between satellites. A European collaborative effort demonstrated a high-speed optical data input and output in free-space between IC chips in computers at a rate of more than 1 Tb/s. Astro Terra, in collaboration with Jet Propulsion Laboratory (Pasadena, CA) has built a 32-channel 1-Ggb/s earth to satellite link with a 2000 km range. Many more active devices in development and some are likely to become crucial components in future optical computer and networks. The race is on with international competitors. NEC (Tokyo, Japan) has developed a method for interconnecting circuit boards optically using Vertical Cavity Surface Emitting Laser arrays (VCSEL). Researchers at Osaka City University (Osaka, Japan) reported on a method for automatic alignment of a set of optical beams in space with a set of optical fibers. As of last year, researchers at NTT (Tokyo, Japan) have designed an optical back plane with free space optical interconnects using tunable beam deflectors and a mirror. The project had achieved 1000 interconnections per printed-circuit board, with throughput ranging from 1 to 10 Tb/s [1].

On other side of view; the future Internet will rely on optical routers without the need for any optoelectronic conversion. Although optical technologies are playing increasingly important roles in wide and local area networks, current optical network elements still offer limited functionality compared to their electronic counterparts. All-optical digital processing is an exciting area of research towards finding new ways to process and transmit information entirely in the optical domain. Optical technology has distinct advantages in the area of transmission of information, e.g. massive bandwidth, absence of electromagnetic interference, and low power consumption. However, its electronic counterpart has the edge in logical processing and switching primarily due to the absence of an equivalent all-optical static memory. Therefore, all-optical digital processing based on bit-serial architecture must been proposed [4].

Though, Optics has a higher bandwidth capacity over electronics, which enables more information to be carried and data to be processed arises because electronic communication along wires requires charging of a capacitor that depends on length. In contrast, optical signals in optical fibers, optical integrated circuits, and free space do not have to charge a

capacitor and are therefore faster. Another advantage of optical methods over electronic ones for computing is that optical data processing can be done much easier and less expensive in parallel than can be done in electronics. Parallelism is the capability of the system to execute more than one operation simultaneously [5].

On the other hand, using a simple optical design, an array of pixels can be transferred simultaneously in parallel from one point to another. To appreciate the difference between both optical parallelism and electronic one can think of an imaging system of as many as 1000x1000 independent points per mm^2 in the object plane which are connected optically by a lens to a corresponding 1000x 1000 points per mm^2 in the image plane. To accomplish this electrically, a million nonintersecting and properly isolated conduction channels per mm^2 would be required. Parallelism, therefore, when associated with fast switching speeds, would result in staggering computational speeds. Assume, for example, there are only 100 million gates on a chip, much less than what was mentioned earlier (optical integration is still in its infancy compared to electronics). Further, conservatively assume that each gate operates with a switching time of only 1 nanosecond (organic optical switches can switch at sub-picosecond rates compared to multi-picosecond switching times for electronic switching). Such a system could perform more than 10^{17} bit operations per second. Compare this to the gigabits (10^9) or terabits (10^{12}) per second rates which electronics are either currently limited to, or hoping to achieve. In other words, a computation that might require one hundred thousand hours (more than 11 years) of a conventional computer could require less than one hour by an optical one [1].

Another advantage of light results because photons are uncharged and do not interact with one another as readily as electrons. Consequently, light beams may pass through one another in full duplex operation, for example without distorting the information carried. In the case of electronics, loops usually generate noise voltage spikes whenever the electromagnetic fields through the loop changes. Further, high frequency or fast switching pulses will cause interference in neighboring wires. Signals in adjacent fibers or in optical integrated channels do not affect one another nor do they pick up noise due to loops. Finally, optical materials possess superior storage density and accessibility over magnetic materials. Obviously, the field of optical computing is progressing rapidly and shows many dramatic opportunities for overcoming the limitations described earlier for current electronic computers. The process is already underway whereby optical devices have been incorporated into many computing systems. Laser diodes as sources of coherent light have dropped rapidly in price due to mass production. Also, optical CD-ROM discs have been very common in home and office computers [2,3,5].

2. Optical Design:

2.1. Metallic Based Design:

The reflectance and transmittance of thin films exhibit strong polarization effects (PEs), particularly for the films inside a glass cube, which result from the fact that the tangential components of the electric and magnetic fields are continuous across each layer interface. This property has been employed in the design of polarizer. However, for some applications it is undesirable and should be reduced. Therefore, the concept and its design methods of non-polarizing beam splitters (NPBSs) are proposed and reported in some literatures. Costich, reported two methods to reduce the PEs in interference films, in 1970, especially in metal–dielectric filters and beam splitters with one air interface [3].

The extension of Costich's theory to the case of a multi-layer inside a glass cube is possible but does not lead to very efficient designs. Mahlein introduced a way to reduce the PEs in two-layer films, while indices of film materials are beyond the value available and it cannot be accepted in practical work. Thelen developed a method of obtaining non-polarizing films in a glass cube by using quarter-wave layers only; however, the region of equal reflectance and transmittance is limited in his solution. Knittl and Houserkova showed a method for synthesizing three-layer equivalent periods with low polarization at oblique incidence. De Sterke et al, developed a design procedure, based on the research of Thelen, using three-layer materials with quarter-wave thickness to achieve NPBSs. Gilo proposed a new design concept, using effective quarter-wave layers of at least three different materials to reduce the PEs on the basis of Brewster condition [3].

All the above apply to the visible part of the spectrum; however, few of the reports on infrared NPBSs can be found, although infrared NPBSs are widely needed. Generally, thin films have strong polarization effects (PEs) at oblique angles of incidence and there will be a difference between the effective indices of p polarization and s polarization, which brings about polarization splitting and reflection-induced retarding. As a very important parameter in polarization optics, reflection induced retarding may cause the change of polarization state of reflected light, which can be simulated digitally. A possible way to solve the problems induced by the reflection-induced retarding is to coat polarization-preserving medium layers on the reflecting surface of the device when the PEs are not desirable. The performance of optical thin films at oblique angles of incidence can be shown to be equivalent to the normal-incidence performance of two designs, one for each polarization. For p polarization, each index of refraction in the design, including the massive media indices, can be replaced by the effective index [3].

2.1.1. Infrared Beam Splitter:

Zheng et al [16], introduce two designs of a ZF-7 or K9 glass cube, which bases on quarter-wave layers at reference wavelength λ = 1300nm and the angle of incidence θ = 45°, show 50% reflectance and 50% transmittance for both polarization states at λ with the measuring error less than 10% and small reflection-induced retarding. For materials Nd2O3, Al2O3 and MgF2, a 14 layers quarter wave stack with alternating high and middle index layers is constructed on the substrate. Then a six layers quarter wave stack with alternating low index and middle index layers is added to the previous stack. It shown that the values of reflectance of p polarization and s polarization at λ = 1300 nm are 50% and 50%, respectively, and the reflection induced retarding is close to zero and reflection induced retarding in the vicinity is very low. For materials ZnS, SiO2 and MgF2, respectively, that the values of the reflectance of p polarization and s polarization at λ = 1300 nm are 43% and 47%, respectively, and the reflection-induced retarding is close to zero [16].

2.1.2. Holographic Optical Element:

Yasuhiro et al [15], suggest a design and fabricate of an optimum holographic optical element (HOE) lens for a femtosecond laser. They design and analyze a HOE lens illuminated with a femtosecond laser pulse. This HOE lens for a laser pulse has 130 fs duration, 720nm central wavelength, and 10nm spectrum bandwidth. The HOE lens gives both high diffraction efficiency and small amount of aberration. The designed HOE lens is fabricated and its optical characteristics have been experimentally evaluated. The reconstructed point images agree with the results of the numerical simulations of the capability of designing the optimum HOE lens for a femtosecond laser pulse [15].

2.1.3. Diffractive Optical Elements:

Xiao et al [14], Design a diffractive optical elements (DOEs) for implementing spatial demultiplexing and spectral synthesizing simultaneously, by using conjugate gradient optimization algorithm. Three different design cases for the spectrum window of the optical communication: three discrete spectral segments in one direction, two discrete spectral segments in two directions, and three discrete spectral segments in three directions, are implemented. The numerical simulations indicate that the designed multi-functional DOEs can successfully generate desired spectra at pre-designed directions. These designs can provide useful information for designing the wavelength division multiplexer and the arrayed waveguide grating in various optical systems. In recent years, diffractive optical elements (DOEs) have been widely used in various optical systems. Because of its small size, light weight, great versatility, and low cost, DOEs become the first choice for laser beam shaping and focusing, spectral synthesizing, laser coupling, correlation filtering, wavelength-division multiplexing, signal processing, optical disk reading out, beam array generating, and so on. Flexible spectrum synthesis now

plays an important role in optical communication system for all optical networks. Most recently, the design of the DOEs is used to synthesize the infrared spectra of real compounds in one direction by several groups [14].

2.2. Organic Based Design:

The photochromic protein bacteriorhodopsin (bR) contained in the purple membrane fragments of Halobacterium halobium, has emerged as an excellent material for bio-molecular photonic applications due to its unique advantages. It exhibits high quantum efficiency of converting light into a state change, large absorption cross section and nonlinearities, robustness to degeneration by environmental perturbations, high stability towards photo-degradation and temperature, response in the visible spectrum, low production cost, environmental friendliness, capability to form thin films in polymers and gels and flexibility to tune its kinetic and spectral properties by genetic engineering techniques, for device applications. By absorbing green–yellow light, the wild type bR molecule undergoes several structural transformations in a complex photocycle that generates a number of intermediate states. The main photocycle of bR is as shown in Fig.1. After excitation with green–yellow light at 570 nm, the molecules in the initial B state get transformed into J state with in about 0.5 ps. The species in the J state thermally transforms in 3 ps into the intermediate K state which in turn transforms in about 2 μs into the L state. From the L state bR thermally relaxes to the MI state within 8 μs and undergoes irreversible transition to the MII state. The molecules then relax through the N and O intermediates to the initial B state within about 10 ms.

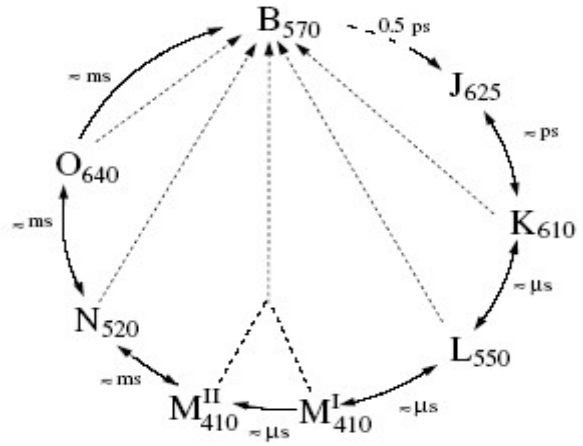

Fig. 1. Schematic of the photochemical cycle of bR molecule. Subscripts indicate absorption peaks in nm. Solid and dashed arrows represent thermal and photo-induced transitions respectively.

An important feature of all the intermediate states is their ability to be photo-chemically switched back to the initial B state by shining light at a wavelength that corresponds to the absorption peak of the intermediate in question. The wavelength in nm of the absorption peak of each species is shown as a subscript in Fig. 1 [9].

Singh et al [9], introduce a simplified level diagram shown in fig.2, to represent the photochemical cycle of bR molecules, which enables adoption of the simple rate-equation approach for the population densities in the various intermediate states. The J state has been neglected in this simplified model, since it has an extremely short lifetime of 3 ps compared to the other states. A single M state (for both spectroscopy identical MI and MII states) and forward transitions between different intermediate states have been considered. They consider bR molecules exposed to a light beam of intensity I_0, which modulates the population densities of different states through the excitation and de-excitation processes [9].

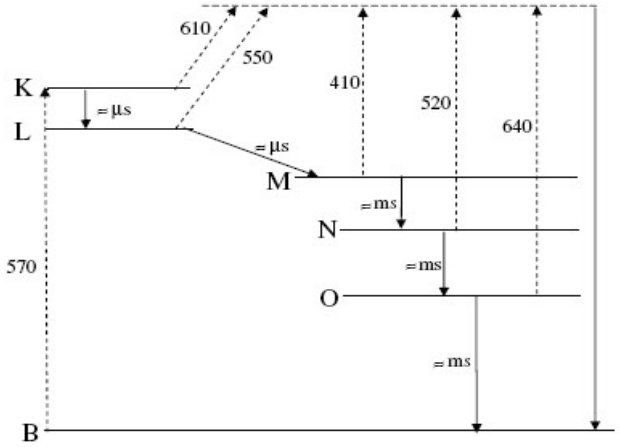

Fig. 2, Simplified level diagram representing the photochemical cycle of bR molecule [5].

2.3. Organ Metallic Based Design:

2.3.1 spatial light modulation:

Serge et al [7], present a general theoretical analysis of all-optical spatial light modulation in organometallic compounds based on nonlinear excited-state absorption, considering the propagation effects of both read and write beams. A detailed analysis for Ptethynyl complex has been presented based on the rate equation approach and an analytical solution for the write beam transmission has been obtained. For typical values, the read beam at 633 nm is modulated by 97.9% with a write beam intensity of 100 kW/cm^2 at 355 nm. It is shown that the effect of write beam propagation in the medium is appreciable at low write beam intensities and the percentage modulation in Ptethynyl complex is larger than that in C60 in toluene and Zn. Spatial light modulation has been analyzed by considering the transmission of a cw read laser beam at 633 nm that corresponds to the He–Ne laser wavelength, through Ptethynyl complex, which is modulated by a cw write laser beam at 355 nm that corresponds to the maximum ground state absorption. An organometallic compound exposed to a light beam of Intensity I(x), which modulates the population densities of different states through the excitation and de-excitation processes. A schematic diagram of

all-optical light modulation of read beam by a write beam in the nonlinear medium is as shown in fig. 3 [7].

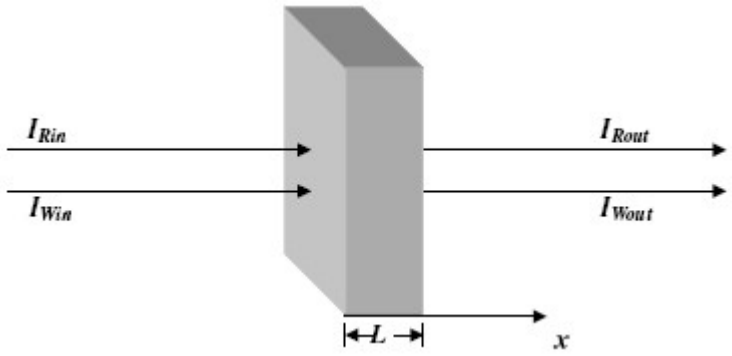

Fig. 3, Schematic diagram of all-optical spatial light modulator [4].

2.3.2. Ptethynyl Thin Film:

Singh et al [8], Introduce a thin film of Ptethynyl complex exposed to a light beam of intensity I, which modulates the population densities of different states through the excitation and de-excitation processes. A schematic diagram of all optical switching of a cw probe beam by a pulsed pump laser beam in the nonlinear medium is as shown in figure 4. These light-induced population changes can be described by the rate equations in terms of the photo-induced and thermal transitions of different levels [8].

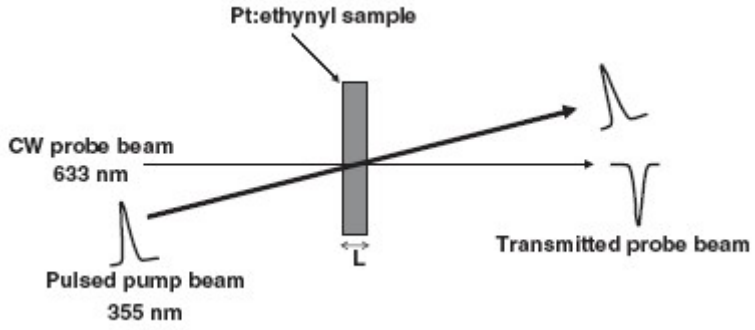

Fig. 4, Schematic diagram of all-optical switching [3].

2.3.3. All-Optical Switching Polymethine Dye:

Prag et al [5], investigate Polymethine dye(2-[2-[3-[(1,3-dihydro-3,3-dimethyl-1-phenyl-2H-indol-2-lidene)ethyline]-2-phenyl-1-cyclohexene -1-yl]ethenyl]-3,3-dimethyl-1-henylindolium perchlorate) (PD3) that exhibits large excited-state absorption, using the rate equation approach, to achieve high contrast and fast switching. The transmission of a cw probe laser beam (I) at 532 nm through PD3 dissolved in (i) ethanol and (ii) polyurethane acrylate (PUA), is switched by a pulsed pump laser beam at 532 and 650 nm, respectively, which excite molecules from the ground state. The theoretical results show good agreement with the reported experimental results for case (i). The switching characteristics have been shown to be sensitive to variation in concentration, pump pulse width, peak pumping intensity and absorption cross-section of the excited-state at 532

nm and lifetime of excited-state. The same switching contrast can be achieved at relatively lower pump powers intensity at 650 nm for case (ii). It is shown that there is an optimum value of concentration at which maximum modulation can be achieved. A 96% modulation of intensity at 650 nm, with t=30 *ps* and concentration of 0.14 mm in PUA, resulting in switch OFF and ON time of 95 *ps* and 18 *ns*, respectively [5].

2.3.4. Phthalocyanine and Polydiacetylene Switching:

Abdeldayem et al [1]; Recently in NASA/Marshall Space Flight Center demonstrated two fast all-optical switches using phthalocyanine thin films and polydiacetylene fiber. The phthalocyanine switch is in the nanosecond regime and functions as an all-optical AND logic gate, fig. 5, while the polydiacetylene one is in the picosecond regime and exhibits a partial all-optical NAND logic gate [1].

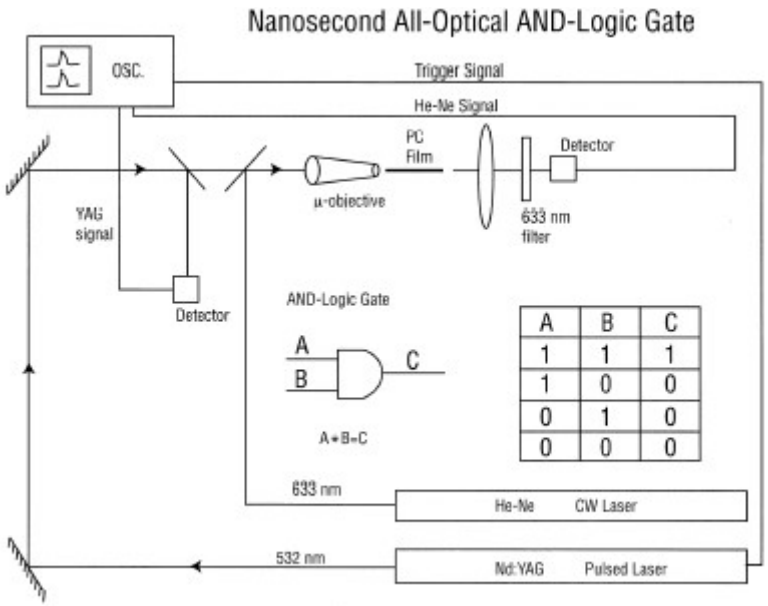

Fig. 5, A schematic of the nanosecond all-optical AND logic gate setup [1].

To demonstrate the AND gate in the phthalocyanine film, they waveguided two focused collinear beams through a thin film of metal-free phthalocyanine film. The film thickness was ~ 1 mm and a few millimeters in length. Then using the second harmonic at 532 nm from a pulsed Nd:YAG laser with pulse duration of 8 ns a long with a cw He-Ne beam at 632.8 nm. The two collinear beams were then focused by a microscopic objective and sent through the phthalocyanine film. At the output a narrow band filter was set to block the 532 nm beam and allow only the He-Ne beam. The transmitted beam was then focused on a fast photo-detector and to a 500 MHz oscilloscope. It was found that the transmitted He-Ne cw beam was pulsating with a nanosecond duration and in synchronous with the input Nd:YAG nanosecond pulse. A schematic of the setup is shown in fig 5. The setup for the picosecond switch was very much similar to the setup in fig. 5 except that the phthalocyanine film was replaced by a hollow

fiber filled with a polydiacetylene. The polydiacetylene fiber was prepared by injecting a diacetylene monomer into the hollow fiber and polymerizing it by UV lamps. The UV irradiation induces a thin film of the polymer on the interior of the hollow fiber with a refractive index of 1.7 and the hollow fiber is of refractive index 1.2. In the experiment, the 532 nm from a mode locked picosecond laser was sent collinearly with a cw He-Ne laser and both were focused onto one end of the fiber. At the other end of the fiber a lens was focusing the output onto the narrow slit of a monochrometer with its grating set at 632.8 nm. A fast detector was attached to the monochrometer and sending the signal to a 20 GHz digital oscilloscope. It was found that with the He-Ne beam OFF, the Nd:YAG pulse is inducing a week fluorescent picosecond signal (40 ps) at 632.8 nm that is shown as a picosecond pulse on the oscilloscope. This signal disappears each time the He-Ne beam is turned on. These results exhibit a picosecond respond in the system and demonstrated three of the four characteristics of a NAND logic gate as shown in fig.6 [1].

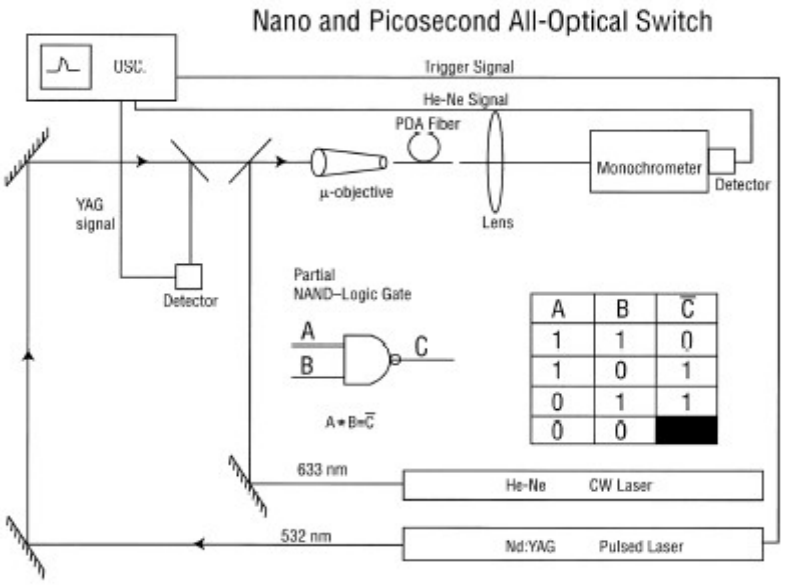

Fig. 6, A schematic of the all-optical NAND logic gate setup [1].

2.4. Semiconductor Optical Amplifier (SOA) Based Design:

2.4.1 NAND Gate Design:

An all-optical NAND gate using integrated semiconductor optical amplifier SOA-based Mach–Zehnder interferometer is proposed by Xiaohua et al [14]. The proposed NAND gate is synchronous with the dynamic gain experienced by the probe pulses. The effects of the SOA and input data parameters on the switching performance are discussed. The operation of the proposed NAND gate with 10 Gb⁄s RZ pseudorandom bit sequences is simulated and the results demonstrate its effectiveness. This NAND gate could provide a new possibility for all-optical routing in future all-optical

networks. In future high-speed optical label-switched networks, optical label will require rapid routing at all-optical switches to avoid cumbersome and power-consuming O/E/O conversion. In transmission, the optical label has to be examined at each node to retrieve the destination information, which is essential for making routing decision [14].

The all-optical high-speed logic gates, which are important for all-optical signal processing such as pattern matching, pseudorandom number generation, and parity checking, may be classified into two categories generally depending on the methodology used to achieve the nonlinear operation of the logic devices, i.e., the fiber nonlinearity based logic gates and the semiconductor-optical-amplifier (SOA)-based logic gates, in which the logic gates employing integrated SOA-based Mach–Zehnder interferometer (MZI) are attractive for simple structure, stable and efficient operation, cascading capability, and easy implementation comparedwith fiber-based devices. The NAND gate has been implemented by nonlinear absorption in Er-doped aluminosilicate glass and semiconductor microresonators. The logic gates based on SOA–MZI configuration is much attractive as it can implement signal regeneration as well.

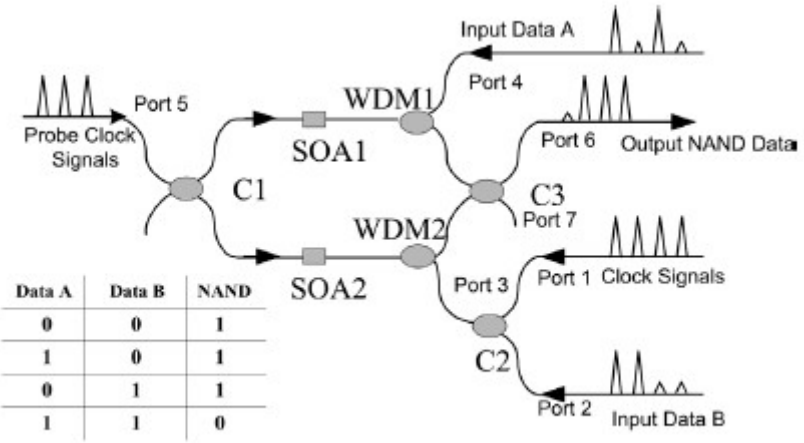

Data A	Data B	NAND
0	0	1
1	0	1
0	1	1
1	1	0

Table 1: Truth table of corresponding NAND

Fig. 7, Schematic diagram of all-optical NAND gate using SOA-MZI [14].

Simulation results show that the scheme can implement all-optical NAND function at 10 Gb/s RZ PRBS input data, which indicates it could be a possible solution for futureall-optical switching applications. Fig. 7, depicts a schematic diagram of the all-optical NAND gate using SOA–MZI. It consisted of a symmetrical MZI with each SOA located in the same relative position of each arm. As control-signals, input data *B* at port 4 are guided into the upper arm of the MZI via a multiplexer WDM1, whereas simultaneous data *A* together with clock pulses combined by coupler C2 enter the lower one via WDM2. Acting as probe signals, clock pulses from port 5 can achieve all-optical3R function and higher extinction ratio compared with CW light. They are divided by the coupler C1 and introduced into two arms of the MZI respectively. The “1” pulses among data *A* and data *B* and the control clock are of the same amplitude [14]. The intensity splitting ratio of all couplers in the scheme is 50/50. With counter-

propagation of the control-signals and the probe pulses, the scheme allows filter-free operation and signal regeneration in the amplitude domain at high bit rates. In operation, the combinations of data *A* and clock signals modulate the carrier density and thereby the refractive index of SOA2 located on the lower arm of MZI, while data *B* works on SOA1 at the upper arm synchronously.

At the output of MZI, the probe signals in both arms interfere either constructively or destructively through coupler C3 depending on the differential phase-shift between two probe pulses, i.e., the input control data determine the phase-shift experienced by the probe pulses, so as to influence the output signal of MZI. When data *A* and data *B* are "1," the control-signals from ports 3 and 4 are identical. Due to the XPM, the differential phase-shift is close to 0, thus the output of MZI becomes 0. In the other cases, the control data from ports 3 and 4 are different, which results in the generation of a pulse at the wavelength of the probe pulses and the output of MZI becomes 1, therefore the logic truth table is achieved [14].

2.4.2. OR Gate Design:

Wang et al[11], demonstrated All-optical OR operation using a semiconductor optical amplifier (SOA) and delayed interferometer (DI) at 80 Gb/s. The DI is based on a polarization maintaining loop mirror. Q-factor of the operation is discussed through numerical simulations. The results show the OR gate operation rate is limited by the gain recovery time and input pulse energy. For high-speed optical communication networks, logic operation is important for networking functions, such as switching, signal regeneration, addressing, header recognition, data encoding and encryption, etc.

All-optical signal processing functionalities are important for some applications where electro-optical conversion is not desired. Recently, optical logic demonstrations using various schemes have been reported. For example, all optical XOR gate using (SOA) based Mach–Zehnder interferometer, and NOR logic gate using two cascaded SOAs has been demonstrated. The NOR function is an OR with an inverter at the output. It is known that a complete logic set can be built with a NOR gate. The inverter function using SOA-delayed interferometer (DI) has been previously demonstrated at speeds of 100 Gb/s and OR function has been demonstrated at 20 Gb/s. They demonstrate SOA-delayed interferometer (DI) based OR function at 80 Gb/s using the gain saturation property of the SOA. Thus, the combination of this work and previous work shows that NOR function, which is important for many applications can be achieved by cascading two sets of SOA-DI devices.

The technique based on SOA-DI devices has the advantage over Mach–Zehnder devices in that it requires one SOA and hence it operates at lower power. The simulation shows the data rate limitation is set by the gain recovery time of the SOA. The OR gate operation is based on the gain

saturation and phase modulation of optical signals in the SOA. The schematic diagram of the principle is shown in fig. 8, The signals A and B and a CWcontrol signal (which would carry the information of OR output) are injected into the SOA, the data signals A and B induce phase shifts to the CW signal via cross-phase modulation in the SOA [11].

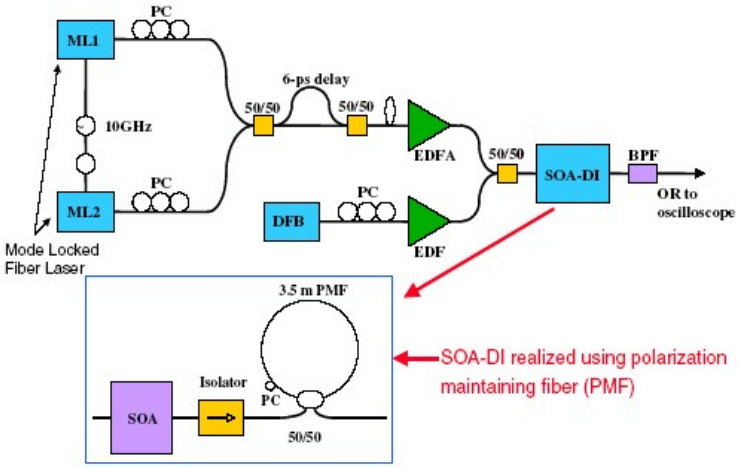

Fig. 8, Experimental setup for the OR function demonstration, ML: mode locked fiber laser, PC: polarization controller, DFB: distributed-feedback laser,BPF: bandpass filter, DCF: dispersion compressing fiber, PMF: polarization maintaining fiber. ML1 and ML2 provide the pulsed sources A and B andDFB laser provides the CW source [11].

The CW signal carrying the time dependent phase shifts is injected into a polarization maintaining loop (PML) mirror, which serves as a delayed interferometer. The input CW signal is polarized along either the fast or the slow axis of the polarization maintaining fiber in the loop prior to injection into the PML. The CW signal splits and propagates in the PML as a clockwise component and a counter clockwise component.

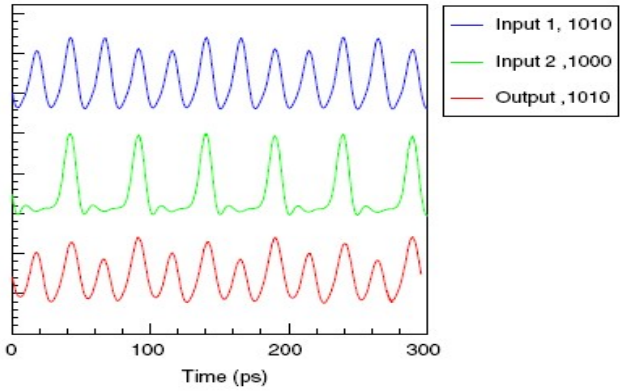

Fig. 9. Experimental result of SOA OR operation [11].

The in-loop polarization controller (which is near the coupler) is adjusted so that it rotates the polarization by 90. Thus, the clockwise component and the counter clockwise component of the light in the PML are polarized along the two optical axis of the polarization preserving fiber. Since the optical path is birefringent, the phase difference between the

pulses with polarization along the fast and slow axis accumulates and results in a differential phase delay of k0, where k0 is the wave vector in the vacuum, Dn is the difference in index seen by the light propagating along the fast and slow axis, and L is the fiber length in the PML. The clockwise and counter clockwise components traverse the in-loop polarization controller once and arrive at the coupler with the same polarization where they interfere [11].

2.4.3. Modular arithmetic processor Design:

Wong et al [12], They present an all-optical processor that is based on the interconnection of low-level logic gates that overall performs modular (or modulo) arithmetic: B / A mod N If A is a positive number and B is between 0 and N, one can think of B as the remainder of A when divided by N. One important application of modular arithmetic is in cryptography. This main scope of this is the logical design of an all-optical processor by interconnecting several low-level logic gates. The modulo-processor has potential application in all-optical packet header processing. The design is based on the bit-serial architecture and consists of SOA logic gates commonly known as TOADs (or sometimes SLALOM) as the main building blocks. The modulo-processor is designed and tested. Fig. 10, demonstrates the basic design of the all-optical modulo-processor [12].

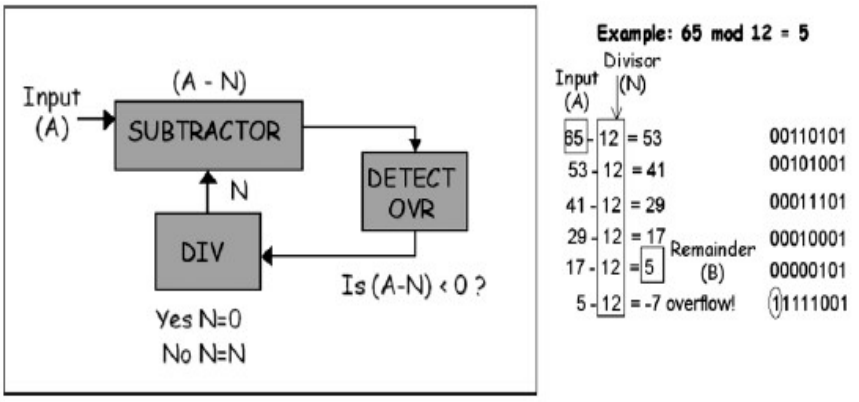

Fig. 10, The basic design of an all-optical modulo-processor that consists of three main modules: (i) subtractor; (ii) divisor; and (iii) detect overflow.

The remainder is defined as the smallest positive number after repeated subtraction. In order to keep track of the sign (±), the most significant bit (MSB) is initially set to '0' so that an overflow could be detected when it becomes '1'. The processing can be done entirely in the optical domain and is made possible by using TOADs as logic and regenerative gates. The interoperation between the all-optical modules within the overall design is shown in fig 11.

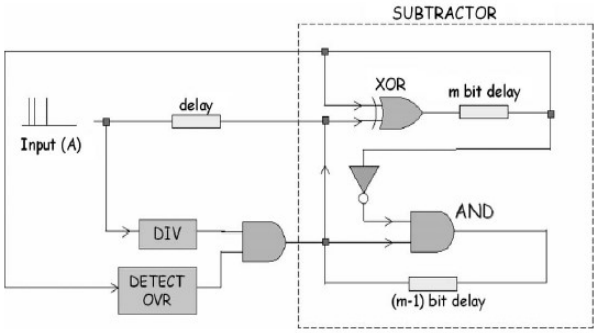

Fig. 11. Logical circuit diagram of the all-optical subtractor module [12].

In the basic design, there are three main modules: (i) subtractor, (ii) divisor, and (iii) detect overflow. The input A is the initial data that enters the subtractor module. Repeated subtraction cycles are performed until the remainder B is computed, i.e. when an overflow (OVR) is detected in the MSB. To perform subtraction, an all-optical subtractor is realized by adding an inverting gate (NOT) to the all-optical full adder. Combiners and TOAD gates are shown in fig 12.

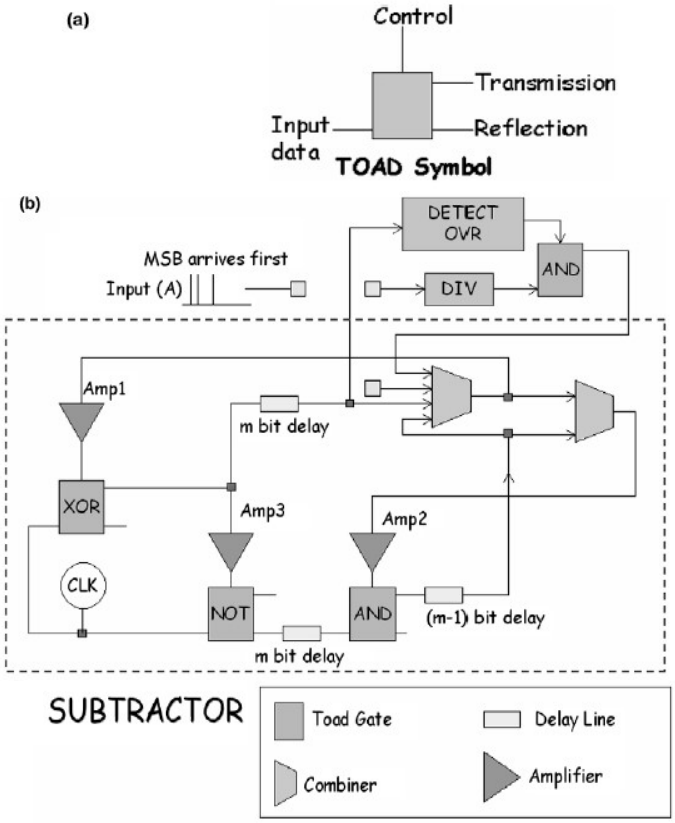

Fig. 12, (a) Symbol of the TOAD module. It requires two input signals (DATA and CTRL) and has two output ports (TRANS and REFL). (b) Optical circuit schematic of the subtractor module [12].

The most complex and costly device will be the TOAD gate, depicted by a four-port symbol. Therefore, the number of such gates should be minimized in the overall design. This saves cost and minimizes complex dynamical interactions. However, the TOAD gates when cascaded in a

feedback configuration have demonstrated some beneficial effects in the form of amplitude restoration. The working principle of the TOAD is based on cross-phase modulation (XPM) between two optical signals. The two input signals can be distinguished from each other by either having different polarization or wavelengths. One of the signals acts as the control pulse while the other is the data pulse. The control pulse imposes XPM on the data pulses through the nonlinear element in the TOAD, which is a SOA. On entry, the data pulses are split into two directions. Then on exit, the data pulse is combined and is either transmitted or reflected depending on the resultant phase difference (due to XPM) between the split data pulses. The SOA parameter values are given in Table 1.

Table 1 Parameter Values of the Semiconductor Optical Amplifier (SOA) [12].

Symbol	Parameters	Values
E_{data} (fJ)	Data pulse energy	10
E_{ctrl} (fJ)	Control pulse energy	400
I_b (mA)	Bias current	173
L (μm)	SOA length	1000
A (μm^2)	Effective cross-sectional area	0.2
Γ	Optical confinement factor	0.3
τ_e (ps)	SOA carrier lifetime	300
A (m^2)	Gain cross-sectional area	2.5×10^{-20}
N_{tr} (m^{-3})	Transparency carrier density	1×10^{24}
n_{eh} (m^3)	SOA nonlinearity	2×10^{-26}
λ (μm)	Operating wavelength	1.55

To realize the XOR gate, allows either 0, 1 or 2 pulses to be present at the control port. if for a phase shift of 2p, the transmission returns to zero then the device would be logically equivalent to an XOR operation (i.e. 0 + 0 = 0, 0 + 1 = 1, 1 + 0 = 1, 1 + 1 = 0). In practice, the saturating gain response makes this not exactly true but it can be close enough for the circuit to function correctly. The reason for this is the ability of the optical gates to reset the logic levels. Point out here that the nonlinear relationship between phase shift and pulse energy is fully included in the simulations. The XOR gate function was demonstrated by slightly delaying the arrival of two control pulses. If cross-gain modulation (XGM) effects are neglected in the TOADs, the best extinction ratio is achieved when the XOR gate is biased at 178 mA while the NOT and AND gates are biased at 173 mA. In reality, XGM effects are present due to a substantial gain difference between the counter propagating pulses, which tend to degrade the switching performance but these effects are neglected for the time being. Also assume that the coupler has perfect 50:50 splitting.

For an SOA with a carrier lifetime (se) of 300 ps, the operating bit rate was chosen to be 1 Gb/s corresponding to a bit period of 1 ns. This limits any pulse-to-pulse interactions that may lead to new dynamical behavior such as spontaneous clock division. Optical amplifiers are required to generate control pulses that have higher energy than data pulses. In the logical design, using the same amplifier for two or more separate branches minimizes amplifier count. Additional all-optical logic gates are also required to form the: (i) DETECT OVR; and (ii) DIV modules fig.13. The

detect-overflow module, shown in fig. 14, consists of four TOAD gates, of which three act as AND gates while the remaining one acts as a D-type flip-flop.

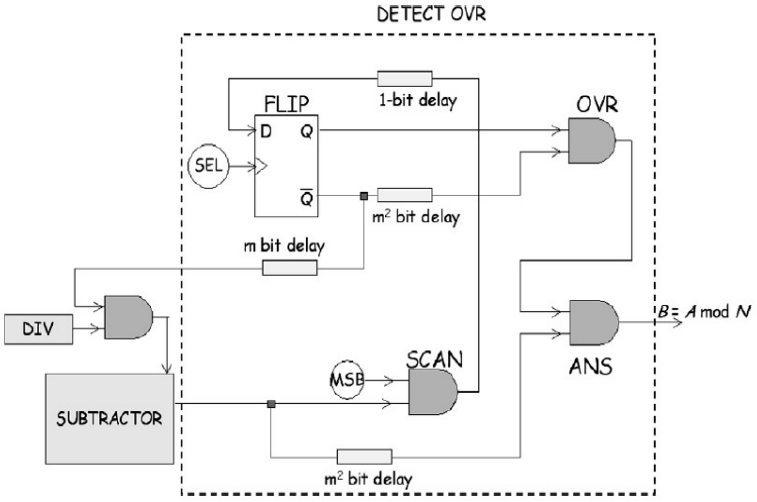

Fig. 13, Logical circuit diagram of the detect-overflow module. The D-type flip-flop is simply a TOAD with a single delay feedback. The remaining three TOAD gates function as AND gates [12].

Two optical clock sources are required, one for the D-type flip-flop and another one for the SCAN(MSB) gate. The clock source into the D-type flip-flop is referred to as the SELECT pattern, which contains m bits of '1 s' followed by m(m - 1) bits of '0s'. This pattern repeats itself every m^2 bits. The clock source into the SCAN gate is referred to as the (scan) MSB pattern and periodically produces a '1' followed by a trail of (m^2-1) bits of '0s'. For example, if m = 8, then an 8-bit operation which would require each subtraction cycle to be equal to m^2 = 64 bits. The flip-flop (FLIP) is implemented by a TOAD gate with a 1-bit delay feedback to itself (see fig. 14) [12].

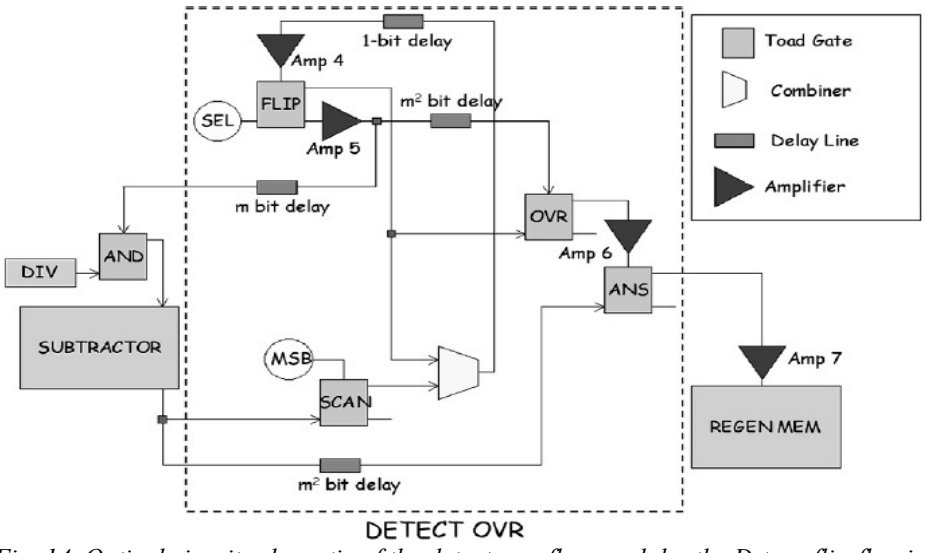

Fig. 14, Optical circuit schematic of the detect-overflow module: the D-type flip-flop is simply a TOAD with a single delay feedback. The remaining three TOAD gates function as AND gate [12].

References:

[1]	Abdeldayem Hossin, Donald O. Frazier, Mark S. Paley, and William K. Witherow, "Photonic Devices for Optical Computing" ,NASA Marshall Space Flight Center, Space Sciences Laboratory, Huntsville, al 35812.
[2]	Kato A., Oishi S., Shishido T., T. Yamazaki T., Iida S., "Evaluation of stoichiometric rare-earth molybdate and tungstate compounds as laser materials", Journal of Physics and Chemistry of Solids 66 (2005) pp.2079–2081.
[3]	Liua W.L.,_, Xiab H.R., Wangb X.Q., Lingb Z.C., Ranb D.G., Xuc J., Weic Y.L., Liua Y.K., Sunb S.Q., Han H., "Characterization of deuterated potassium dihydrogen phosphate single crystals grown by circulating method", Journal of Crystal Growth 293 (2006) pp.387–393.
[4]	Nandigana Krishna Mohan, Quazi T. Islam, "Design of an off-axis HOE light concentrator to focus light from multiple directions in a plane" , Science Direct, Optics and Lasers in Engineering 44, (2006), pp943–953.
[5]	Parag Sharma, Sukhdev Roy, C.P. Singh, "Dynamics of all-optical switching in polymethine dye molecules", Science Direct, Thin Solid Films 477, (2005), pp42– 47.
[6]	Richard Scheps, "Upconversion Laser Processes", SSDI:007/727, frog. Quanr. Elecrr. 1996. Vol. 20. No. 4 pp.271-358,Published by Elsevier Science Ltd, Printed in Great Britain.
[7]	Serge Gauvin, Joseph Zyss, "Growth of organic crystalline thin films, their optical characterization and application to non-linear optics", Journal of Crystal Growth 166 (1996) pp.507-527
[8]	Singh C.P., Kapil Kulshrestha, Sukhdev Roy, "High-contrast all-optical switching with Pt:ethynyl complex", Optics , ww.sciencedirect.com.
[9]	Singh C.P., Sukhdev Roy, "All-optical logic gates with bacteriorhodopsin", Science Direct, Current Applied Physics 3, (2003), pp163–169.
[10]	Stefan A. Amarande, Michael J. Damzen, "Measurement of the thermal lens of grazing-incidence diode-pumped Nd:YVO4 laser amplifier", Optics Communications 265 (2006) pp.306–313.
[11]	Wang Q., Dong H., Zhu G., Sun H., Jaques J., Piccirilli A.B., Dutta N.K., "All-optical logic OR gate using SOA and delayed interferometer", Optics Communications 260 (2006) pp.81–86
[12]	Wong W.M., Blow K.J., "Design and analysis of an all-optical processor for modular arithmetic", Optics Communications (2006)
[13]	Xiao dong Sun, Juan Liu, Yi-quan Wang, Bo Zhang, Bin Hu, Si Di, Shang Wang, "Diffractive optical elements for implementing spatial demultiplexingand spectral synthesizing simultaneously", Optics Communications (2006)

[14]	Xiaohua Ye, Peida Ye, Min Zhang, "All-optical NAND gate using integrated SOA-based Mach–Zehnder interferometer", Optical Fiber Technology, www.ScienceDirect.com.
[15]	Yasuhiro Awatsuji, Yuu Shiuchi,Aya Komatsu, Toshihiro Kubota, "Design and fabrication of an Optimum holographic optical element lens for a femtosecond laser pulse using a hologram computer-aided design tool ", Optics and Lasers in Engineering 44 (2006) 975–990.
[16]	Zheng Ping Wang_, Jin Hui Shi, Shun Ling Ruan, "Designs of infrared non-polarizing beam splitters", Optics & Laser Technology 39 (2006) pp.394–399.